Annals of Biomedical Engineering, Vol. 39, No. 9, September 2011 (© 2011) pp. 2445–2455
DOI: 10.1007/s10439-011-0331-4

Inelasticity of Human Carotid Atherosclerotic Plaque

EOGHAN MAHER,[1] ARTHUR CREANE,[2] SHERIF SULTAN,[3,4] NIAMH HYNES,[3,4] CAITRÍONA LALLY,[2] and DANIEL J. KELLY[1]

[1]Trinity Centre for Bioengineering, School of Engineering, Trinity College, Dublin, Ireland; [2]School of Mechanical and Manufacturing Engineering, Dublin City University, Glasnevin, Dublin 9, Ireland; [3]Western Vascular Institute, Department of Vascular & Endovascular Surgery, University College Hospital Galway, Galway, Ireland; and [4]Department of Vascular & Endovascular Surgery, Galway Clinic, Doughiska, Dublin Road, Galway, Ireland

(*Received 3 December 2010; accepted 17 May 2011; published online 27 May 2011*)

Associate Editor Peter E. McHugh oversaw the review of this article.

Abstract—Little mechanical test data exists regarding the inelastic behavior of atherosclerotic plaques. As a result finite element (FE) models of stenting procedures commonly use hyperelastic material models to describe the soft tissue response thus limiting the accuracy of the model to the expansion stage of stent implantation and leave them unable to predict the lumen gain. In this study, cyclic mechanical tests were performed to characterize the inelastic behavior of fresh human carotid atherosclerotic plaque tissue due to radial compressive loading. Plaques were classified clinically as either mixed (M), calcified (Ca), or echolucent (E). An approximately linear increase in the plastic deformation was observed with increases in the peak applied strain for all plaque types. While calcified plaques generally appeared stiffest, it was observed that the clinical classification of plaques had no significant effect on the magnitude of permanent deformation on unloading. The test data was characterized using a constitutive model that accounts for both permanent deformation and stress softening to describe the compressive plaque behavior on unloading. Material constants are reported for individual plaques as well as mean values for each plaque classification. This data can be considered as a first step in characterizing the inelastic behavior of atherosclerotic plaques and could be used in combination with future mechanical data to improve the predictive capabilities of FE models of angioplasty and stenting procedures particularly in relation to lumen gain.

Keywords—Mechanical properties, Plastic deformation, Permanent deformation, Stress softening, Plaque, Constitutive model.

INTRODUCTION

Atherosclerosis is a disease of arteries which commonly results in a reduction of lumen area, caused by a build up of fatty material in the artery wall, and a corresponding decrease in blood flow through the diseased artery. Common treatments for these stenosed arteries include balloon angioplasty, stenting or a combination of the two. The objective of these procedures is to increase the lumen size through mechanical loading of the stenosed artery. Little is known, however, about the inelastic mechanical behavior of atherosclerotic plaques and its contribution to lumen gain. A number of authors have investigated the response of atherosclerotic plaques to different loading regimes.[3,11,18,22,23,27,28,42] The characterization of the response to mechanical testing has most commonly been undertaken using hyperelastic material models to describe the effects of monotonic uniaxial loading.[28] To the author's knowledge, Topoleski and coworkers[42,43] are the only researchers to report specifically on the inelastic behavior of atherosclerotic plaques. In this study, the response of the plaques to successive cyclic compression loading regimes and successive stress relaxation loading regimes, with unloaded "rest" periods in each case, was investigated. The degree of recovery in the mechanical properties during the "rest" periods was found to depend on the plaque type, with calcified plaques reported as behaving more elastic than other types. However, further mechanical testing is needed to characterize atherosclerotic plaque response adequately for use in finite element (FE) analyses; in particular the inelastic behavior needs to be quantified across a wide range of applied strains in order to develop appropriate inelastic material models.

In order to accurately describe a material's mechanical behavior the development of any constitutive model requires relevant mechanical testing data. Due to the lack of inelastic data discussed above hyperelastic constitutive models are often used in FE

Address correspondence to Daniel J. Kelly, Trinity Centre for Bioengineering, School of Engineering, Trinity College, Dublin, Ireland. Electronic mail: kellyd9@tcd.ie

analysis of stenting procedures[5,10,21,26,30,31,37] in diseased arteries to assess and improve stent performance and design. Others have additionally investigated the artery behavior on unloading such as lumen gain post-stenting.[9,20,48] As such models do not consider any inelastic behavior they are unable to accurately quantify lumen gain post-angioplasty or stenting.

There are few models available in the literature to describe inelastic behavior of soft tissues such as arteries and plaques. The inelastic effects commonly investigated include softening similar to the Mullins effect[4,35,36] and plastic deformations.[13,40] The softening models are commonly based on continuum damage mechanics[16,29,39] or on pseudo-elastic[8,34] approaches proposed for rubber-like materials. Calvo *et al.*[4] proposed an uncoupled anisotropic damage model for fibered biological soft tissues, where damage was defined separately for the matrix and the fibers of the material. Their approach applied continuum damage mechanics to describe irreversible Mullins like softening to the fibers and matrix separately. Pena *et al.*[35] proposed a similar model that introduced a further viscoelastic approach that described the hysteresis in fibered soft tissues, while Balzani *et al.*[2] applied damage to the fiber direction components only. Volokh and Vorp[44] extended the typical softening hyperelastic theory to include a constant to describe the maximum possible energy that a material can accumulate before failure occurs. A number of other models have been proposed to model the softening behavior of soft tissues.[12,16,25] Gasser and Holzapfel[13] developed a rate-independent elasto-plastic constitutive model for fiber-reinforced biological tissues. They use the concept of multi-surface plasticity as the basis of their constitutive framework to induce plastic deformations in the tissue. Gasser and Holzapfel[14] used this model to describe the media in a FE analysis of a balloon angioplasty. In this study, the plaque was modeled as a rigid body and the inelastic constants for the media were assumed presumably due to the unavailability of suitable mechanical test data for the inelastic behavior of vascular soft tissue. Other studies[25,49] have used multi-mechanism models where damage is introduced in the elastin and collagen separately, and a residual strain results when the elastin fails. Alternative approaches to incorporating plastic deformations involve approaches based on pseudo-elasticity[8] and network alterations of chain models.[7]

The objective of this study is to determine the inelastic radial compressive behavior of human carotid atherosclerotic plaque. The inelastic mechanical properties of the plaque tissue were investigated using a cyclic radial compressive loading regime. This regime allowed the altered stress–strain behavior resulting from increasing strain in the load history of the tissue to be observed and the residual plastic deformations in the tissue to be quantified. In order to concisely describe the observed experimental phenomena, we present a phenomenological constitutive model incorporating inelastic effects. The model has been adapted from a basis in pseudo-elastic theory. Such analysis should be seen as a first step toward the complete characterization of the inelastic behavior of atherosclerotic plaque. It is believed that this data, when combined with further tensile test data, could be used to improve the predictive ability of FE models and hence aid in the optimization of stent designs in order to achieve maximum lumen gain post-stenting.

MATERIALS AND METHODS

Constitutive Model

An isotropic phenomenological constitutive model was implemented that incorporates the inelastic behavior of vascular soft tissue, including plastic deformations and softening effects. The proposed constitutive relationship can be expressed in terms of the Cauchy Stress, σ,

$$\sigma = (1 - D)(\sigma_{IL} - \sigma_{IN}) \tag{1}$$

where

$$\sigma_{IL} = 2J^{-1}F\frac{\partial W_{IL}}{\partial C}F^{T} \quad \text{and} \quad \sigma_{IN} = 2J^{*-1}F^{*}\frac{\partial N}{\partial C^{*}}F^{*T} \tag{2}$$

F, J, and C are the deformation gradient tensor, the Jacobian determinant, and right Cauchy-Green strain tensor, respectively. F^*, J^*, and C^* are the values of the deformation gradient tensor, Jacobian determinant, and right Cauchy-Green strain tensor calculated when the deformation in the load history of the material is at a maximum. σ_{IN}, the inelastic stress tensor, generally behaves as a constant that reduces the stress in the material. σ_{IL}, the initial loading stress tensor, is a stress tensor calculated by differentiating a strain energy density function, W_{IL} with respect to the right Cauchy-Green strain tensor. The constant tensor σ_{IN} is updated when certain criteria, discussed later, are met that result in the evolution of the function N. If the material is loaded in any direction, a residual or plastic strain will result on unloading to the zero-stress state.

W_{IL} is the strain energy density of the theoretical undamaged, or elastic, material and is equal to the strain energy during initial loading. W_{IL} is a function of the right Cauchy-Green strain tensor C and is expressed in Eq. (3) as an exponential function of the

first principle invariant of C, I_1 as proposed by Delfino *et al.*[6]

$$W_{IL}(C) = W_{IL}(I_1(C)) = \frac{a}{b}\left(\exp\left(\frac{b}{2}(I_1 - 3)\right) - 1\right), \tag{3}$$

where a and b are material constants. It should be noted that any number of commonly used isotropic constitutive models could potentially be used to fit to this data.

N is a function of the right Cauchy-Green strain tensor of the material at its peak deformation in the loading history, C^* and results in inelastic behavior on unloading. N is described below as a function of the first principle invariant of C^*,

$$N(C^*) = c^*(I_1^* - 3), \tag{4}$$

where c^* is a material constant. N only evolves under certain criteria described below.

The peak deformation state is defined here as the deformation state at which W_{IL} is a maximum. This leads to the first criterion, for which the function N can evolve, where

$$\phi = W_{IL} - \alpha \leq 0, \quad \text{and} \quad \alpha(t) = \max_{s\in[0,t]} W_{IL}(s) \tag{5}$$

and α is the maximum value of W_{IL} during the history time interval $[0,t]$. The second criterion for the evolution of N is that C^* is only updated on unloading from the maximum deformation state. This second criterion can be accounted for in a similar method as in the discussion of isotropic damage in hyperelastic materials by Naghdi and Trapp.[32] $\dot{W}_{IL} < 0$ describes unloading of the material. Thus, the criteria for evolution of C^* and hence N and σ_{IN} is given below

$$\text{if} \quad \phi = 0 \quad \text{and} \quad \dot{W}_{IL} < 0, \qquad C^* = C \tag{6}$$

The initial value of C^* is the identity tensor as no deformation has occurred. This results in the initial value of N being zero. Thus, during initial loading the material response is described purely by W_{IL} as stated previously in this section.

The $(1 - D)$ term in Eq. (1) introduces a stress softening factor to the model that allows the constitutive response of the model to better fit to the stress–strain behavior on unloading of the material observed experimentally in this study. D is called the softening parameter and is a function of the maximum and current values of the function W_{IL}.

$$D(\alpha(t), W_{IL}(C)) = \zeta_\infty\left(1 - e^{\frac{-(\alpha(t) - W_{IL}(C))}{i}}\right), \tag{7}$$

where ζ_∞ and i are material constants and $\alpha(t)$ is the maximum value of W_{IL} in the loading history as described in Eq. (5). As the material is initially loaded $\alpha(t) = W_{IL}(C)$ which implies that $D = 0$ and that the stress softening factor has no effect on the stress in the material. The material elasticity tensor $\mathbf{C}$ (Eq. 8) can be found using the product and chain rules for differentiation and the assumption that the inelastic stress tensor is not dependent on the current deformation of the material.

$$\mathbf{C} = \begin{cases} (1 - D)\mathbf{C}_{IL} & \text{if } \phi = 0 \text{ and } \dot{W}_{IL} > 0 \\ (1 - D)\mathbf{C}_{IL} - \frac{\partial D}{\partial W_{IL}} S_{IL} \otimes S_{IL} + \frac{\partial D}{\partial W_{IL}} S_{IL} \otimes S_{IN} & \text{otherwise} \end{cases} \tag{8}$$

where

$$\mathbf{C}_{IL} = 2\frac{\partial S_{IL}}{\partial C} \quad S_{IL} = JF^{-1}\sigma_{IL}F^{-T} \quad S_{IN} = JF^{-1}\sigma_{IN}F^{-T} \tag{9}$$

Mechanical Testing

Cyclic compressive tests were performed on samples taken from plaques of the carotid bifurcation. Plaque specimens were removed from eight patients (five men and three women, 66.13 ± 9.13 years, mean ± SD) during routine carotid endarterectomies. All surgeries and tests were performed in the Galway Clinic, Ireland. The study includes 21 compressive samples obtained from eight carotid plaques. Table 1 includes all patient and lesion details. Plaque classifications were determined independently by a clinician using routine Duplex ultrasound with gray scale imaging.[33,41] Ethical approval for testing of the human tissue was obtained prior to commencing this study from the Galway Clinical Ethics board.

Sample Preparation

Plaque specimens were prepared for testing immediately following removal in surgery. Specimens were dissected at the bifurcation, separating them into common, internal and external carotid segments as described in Maher *et al.*[28] Each segment was opened by cutting along the axial direction. 4-mm diameter cylindrical radial compressive samples were removed from each of the flat rectangular segments using stainless steel punches. Testing samples were allowed to equilibrate in 0.9% saline solution for approximately 30 min before measurements of the sample dimensions were recorded.

Testing Conditions

Testing was performed using a computer controlled, high precision testing device adapted for

TABLE 1. Patient/specimen details.

Specimen	Gender	Age (yr)	Clinical classification	No. of samples
1	Male	83	Calcified proximally, mixed distally	2
2	Female	71	Mixed	2
3	Male	65	Mixed, mostly echolucent	5
4	Male	61	Calcified	3
5	Female	63	Mostly calcified, echolucent at the origin	2
6	Male	73	Calcified proximally, mixed distally	2
7	Male	58	Mixed	3
8	Female	55	Calcified proximally, mixed distally	2
	Age, mean ± SD (yr)	66.13 ± 9.13	Total no. of samples	21

testing biological specimens (Bose ElectroForce 3100, Bose Corporation, Gillingham, UK). The testing rig has an electromagnetic driven motor, with a stroke resolution of 0.0015 mm, a maximum stroke length of 5 mm, and a minimum load resolution of 6 mN with a 22 N load cell. Samples were tested inside a water bath filled with 0.9% saline solution in order to maintain sample hydration during testing. All samples were tested at room temperature within 2 h of harvesting.

Unconfined cyclic compression tests were performed on cylindrical compressive samples. A sample was placed on the lower platen and the upper platen was moved to apply a small compressive pre-load of 0.01 N to the sample at a crosshead speed of 0.001 mm/s. This ensured a consistent contact between the platen and the top of the sample and minimal strain in the plaque, $<5\%$ in all cases. The sample height was then taken as the distance between the platens at this pre-load. Loading was under strain control and several strain levels were applied with five loading–unloading cycles for each loading level. Samples were loaded and unloaded at a rate of 5% strain/s. The loading levels were between 10 and 50% strain in 10% increments and unloading was to the 0% strain level in each case, see Fig. 1. This testing methodology is similar to that used to determine stress softening in rubbers.[24,47] Preliminary testing was performed on porcine arterial tissue in an attempt to rule out possible visco-elastic or poro-elastic response of the tissue. A resting period of 2 h at 0% strain was added every five cycles before the peak strain value was increased. No significant difference was found between the levels of inelastic deformation on unloading between arterial samples tested with or without the relaxation period present. This indicates that no significant recovery of the tissue occurred which suggests that the inelastic response was in line with the theoretical concept presented here.

Data Fitting and Analysis

The data fitting assumes that homogeneous deformation occurred in the tissue during uniaxial loading.

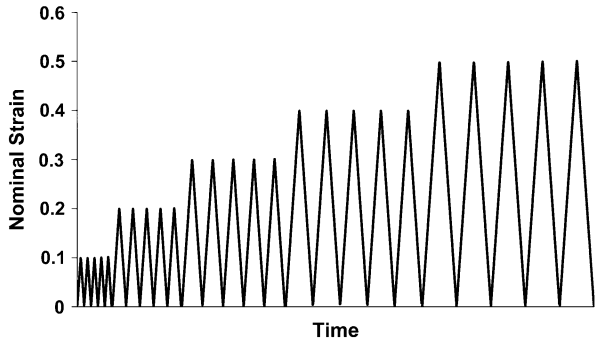

FIGURE 1. Cyclic loading applied to samples.

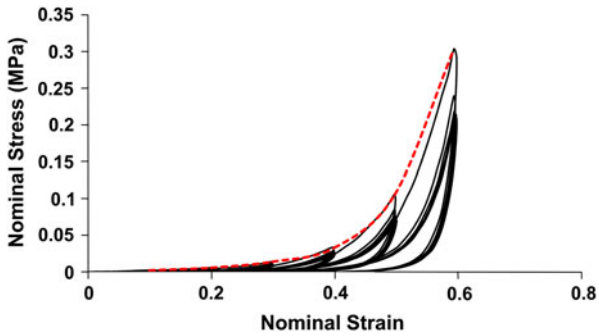

FIGURE 2. Typical response of atherosclerotic plaque to cyclic testing (sample 8(ii)). Dotted line represents the theoretical "load envelope" of the tissue.

A typical stress–strain response of atherosclerotic plaque is seen in Fig. 2. The *loading envelope* is defined as a curve composed of the peak stress–strain points of each strain level (see Fig. 2). These points are the maximum stress–strain points in the first cycle at each new strain level. It has been observed in rubbers that the monotonic loading behavior of a material is similar to this loading envelope.[24] As the variable nature of atherosclerotic plaque properties (as seen in a previous study[28]) rules out testing monotonic and cyclic behavior separately, the loading envelope is assumed to be indicative of the plaque's monotonic loading behavior. The function W_{IL} is fit to the

loading envelope using a linear least squares procedure. The fitting of the load envelope is similar to the fitting process used in a previous study[28] and aims to minimize the relative error between the nominal uniaxial stress predicted by W_{IL} using Eq. (10) and that measured experimentally to obtain the constants a and b. The nominal stress of an incompressible material during initial uniaxial loading, T_{IL}, can be expressed as[17]:

$$T_{IL} = \frac{\partial W_{IL}}{\partial \lambda} = 2(\lambda - \lambda^{-2})\frac{\partial W_{IL}}{\partial I_1}, \tag{10}$$

where λ is the uniaxial stretch the material has undergone in the direction of loading.

The next step is to determine the material parameter c^* by fitting to the permanent deformations experienced at different levels of peak strain. A function, T_P, for nominal stress in an incompressible material with permanent deformations is defined as:

$$\begin{aligned} T_P &= \lambda^{-1}\sigma \\ &= \lambda^{-1}\left[2(\lambda - \lambda^{-2})\left(\lambda\frac{\partial W_{IL}}{\partial I_1}\right) - 2\left(\lambda^* - \lambda^{*-2}\right)\left(\lambda\frac{\partial N}{\partial I_1^*}\right)\right], \end{aligned} \tag{11}$$

where λ^* is the maximum stretch that has occurred in the loading direction in the load history. The current stretch, λ, at which T_P is equal to zero gives the predicted plastic deformation for a given value of λ^*. A linear least squares procedure is utilized to find the value of the parameter c^* that results in the minimum combined relative error between plastic deformation predicted using Eq. (11) and that experimentally measured for all load levels.

The final step in the data-fitting procedure is to use the softening parameter D to improve the accuracy of the unloading and reloading behavior predictions of the model. As the majority of the inelastic effect is seen to occur in the first load–unload cycle of each peak strain level while the subsequent reloading and unloading curves are nearly superimposed, see Fig. 2, the second loading curve in each cycle is assumed to represent the materials unload and reload behavior. A linear least squares procedure is utilized to find the value of the parameters ζ_∞ and i, by minimizing the total relative error between experimental stress–strain response observed on reloading and that predicted by the model for all the peak loading levels. The nominal stress predicted by the model for a uniaxially loaded incompressible material, T (Eq. 12), is utilized in this step using the values for a, b, and c^* calculated in previous steps.

$$T = (1 - D)(T_P) \tag{12}$$

As an independent measure of the quality of the constitutive model fit the root mean square error χ was used (Eq. 13).

$$\chi = \sqrt{\frac{\sum_i (\text{data measured } (i) - \text{data calculated } (i))^2}{n - q}}, \tag{13}$$

where n is the number of data points and q is the number of constants to be fit. Each of the three fits described above (i.e., initial loading, magnitude of permanent deformation, and the unloading–reloading response) were analyzed separately. The average of the two errors concerning the stress–strain response, χ_s, and the error for the permanent deformation fit, χ_{pd}, are reported in Table 2. The experimental data were analyzed to investigate any variation in the inelastic behavior of atherosclerotic plaques due to their clinical classification (calcified, echolucent, and mixed).

RESULTS

Test Data

The stress–strain response of a typical mixed classification plaque is shown in Fig. 2. This graph is representative of the behavior seen in all of the plaque classifications in response to the applied cyclic loading; there is a large softening effect observed between the first loading cycle in each strain level and the subsequent cycles where the response is much more consistent. Plastic deformation that increases with the peak applied load can also be observed. Differences in the loading and unloading response of the plaques indicate a hysteresis effect. The unloading response of the tissue is consistent for all cycles in each level of applied strain.

There is an approximately linear increase in the plastic deformation occurring on unloading with increases in the peak applied strain in the plaques, see Fig. 3. This approximately linear relationship is observed for all three plaque types. The magnitude of plastic strain on unloading from a given applied strain is relatively consistent for each plaque classification. For example, on unloading from 30% strain there is a residual plastic strain of between 9 and 12.5% in echolucent plaques, illustrating the relatively low variability in plastic strain. The magnitude of plastic strain also does not appear to be significantly affected by the type of plaque, see Fig. 3d.

Constitutive Model Data Fitting

The fitted constitutive material constants for each of the plaque specimens are reported in Table 2. The

TABLE 2. Constitutive model material constants fitted to experimental cyclic compression data.

Sample	Classification	a (kPa)	b	C^* (kPa)	ζ_∞	i	χ_s (MPa)	χ_{pd}
1(i)	Ca	70	0.5	11	0.9	0.03	0.041	0.0242
1(ii)	M	4.5	0.25	0.62	0.9	0.004	0.0052	0.0151
2(i)	M	23	0.7	4.5	0.95	0.03	0.017	0.022
2(ii)	M	1.9	0.0001	0.35	0	NA	0.0008	0.002
3(i)	M	55	0.44	11.5	0.9	0.01	0.042	0.024
3(ii)	E	15.7	0.415	2.8	0.87	0.008	0.081	0.0074
3(iii)	E	27	0.925	6.2	0.92	0.007	0.0215	0.021
3(iv)	E	4.2	0.25	0.66	0.95	0.008	0.002	0.008
3(v)	E	11.5	1.165	2.1	0.91	0.014	0.019	0.006
4(i)	Ca	93	1.88	17.5	0.85	0.045	0.083	0.022
4(ii)	Ca	10	0.62	1.8	0.9	0.008	0.0055	0.0124
4(iii)	Ca	18	1.29	4.4	0.95	0.008	0.01	0.011
5(i)	Ca	47	0.747	12	0.97	0.009	0.029	0.038
5(ii)	E	2.5	0.6	0.45	0.87	0.002	0.0007	0.0123
6(i)	Ca	40	5.3	5	0.65	0.01	0.042	0.012
6(ii)	Ca	120	4.35	26.9	0.85	0.011	0.116	0.0096
7(i)	M	100	0.5	14.5	0.92	0.018	0.052	0.018
7(ii)	M	80	0.6	11	0.9	0.017	0.041	0.0233
7(iii)	M	110	4.2	26	0.7	0.01	0.093	0.023
8(i)	Ca	150	1.22	28	0.84	0.015	0.026	0.0224
8(ii)	M	9	1.72	2	0.9	0.01	0.008	0.0095
Overall	Mean ± SD	47.25 ± 45.32	1.32 ± 1.47	9.01 ± 9.04	0.838 ± 0.207	0.014 ± 0.01	0.035 ± 0.033	0.016 ± 0.008
Calcified	Mean ± SD	68.5 ± 49.49	1.99 ± 1.82	13.33 ± 10.04	0.864 ± 0.099	0.017 ± 0.013	0.044 ± 0.038	0.019 ± 0.01
Echolucent	Mean ± SD	12.18 ± 9.87	0.67 ± 0.37	2.44 ± 2.32	0.904 ± 0.034	0.008 ± 0.004	0.025 ± 0.033	0.011 ± 0.006
Mixed	Mean ± SD	47.93 ± 44.38	1.05 ± 1.37	8.81 ± 8.81	0.771 ± 0.321	0.014 ± 0.008	0.032 ± 0.031	0.017 ± 0.008

M—mixed, Ca—calcified, E—echolucent.

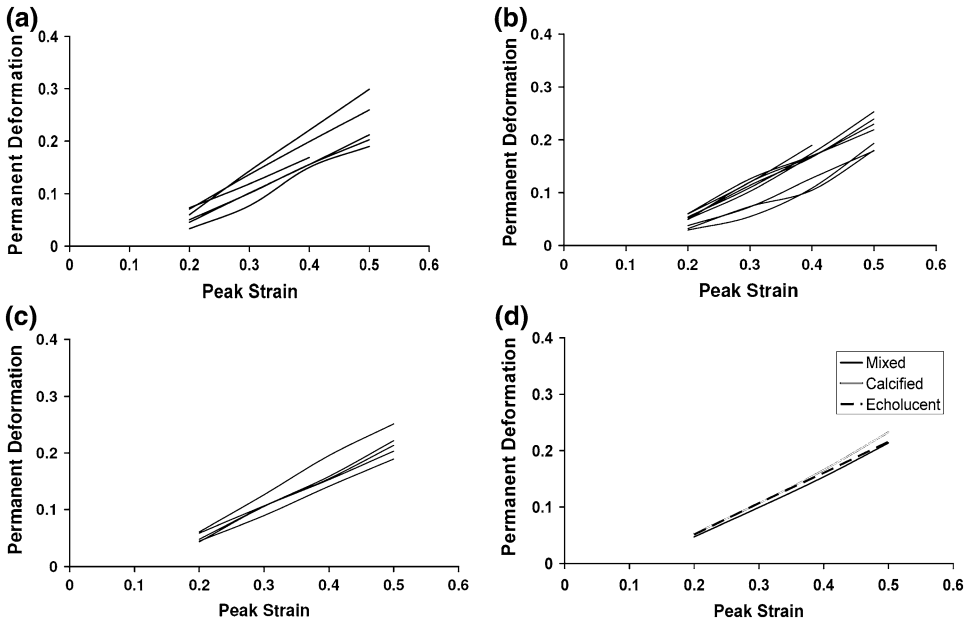

FIGURE 3. Plastic strain at different applied peak strains for the plaque specimens grouped by clinical classification; (a) calcified; (b) mixed; (c) echolucent; (d) shows the mean plastic strain for given applied strains for each classification.

mean constants for each plaque classification are similarly reported. The mean values of the constants a and b, which represent the initial loading behavior and uniaxial loading response of the plaques, suggest that, similar to the trend observed previously[28] the calcified plaques are on average the stiffest plaque type, while the echolucent plaques are the least stiff. However, the large standard deviations illustrate that there is

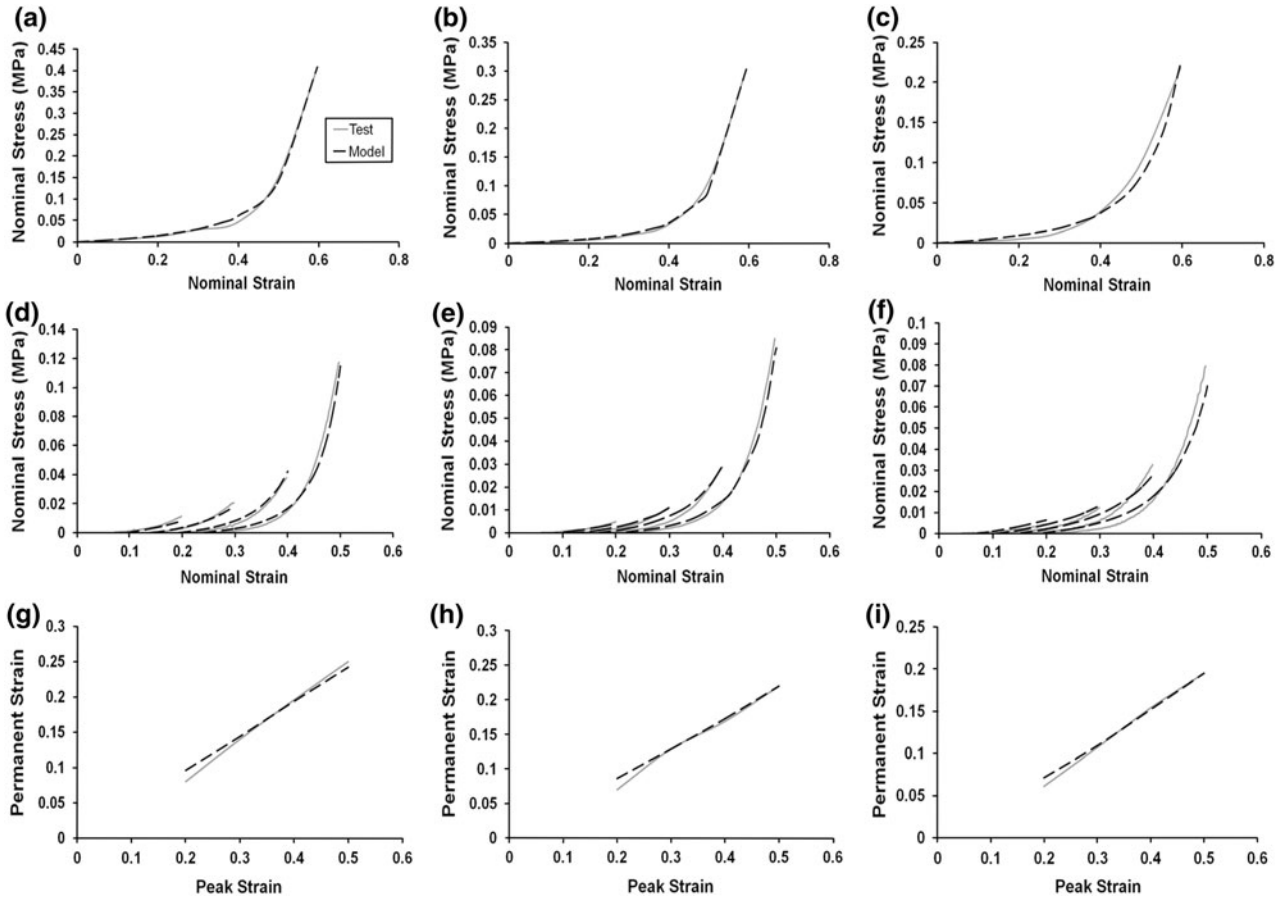

FIGURE 4. Constitutive model fit (dashed black line) to experimental data (gray line) for the load envelope of representative calcified (a), mixed (b), and echolucent (c) plaques; the second loading cycle of each strain level of each of the representative plaques [(d), (e), and (f), respectively]; and the magnitude of residual strains on unloading for given applied strains [(g), (h), and (i), respectively]. The residual strain predicted by the model on unloading is equivalent to the zero-stress state.

significant variation in the uniaxial loading behavior of each plaque type. A relatively smaller magnitude of variability is observed in the inelastic constants, ζ_∞ and i of the softening parameter.

The ability of the constitutive model used to describe the inelastic behavior of the representative plaque behavior for calcified, echolucent, and mixed plaque classifications is illustrated in Fig. 4. The initial loading behavior of the plaque, the reloading curves, and the magnitude of plastic strain predicted by the model for each strain level are seen to adequately approximate the behaviors observed in the mechanical tests.

DISCUSSION

In this article, the inelastic behavior of human carotid plaques in response to radial compression was investigated through mechanical testing. The inelastic effects observed in soft tissues include stress softening and plastic deformations similar to what is observed in rubbers,[7,8] and both phenomena were observed for carotid plaques here. Interestingly, it was observed that plaque composition had no significant effect on the magnitude of permanent deformations occurring on unloading of the plaque. It might be expected that plaques of different composition whose loading behavior tends to be dependent on plaque type[18,28] would experience different unloading responses. However, it is possible that different mechanisms of damage may be more prevalent in each plaque type, leading to similar end results. Clinical studies[15] have reported no significant difference in acute lumen gain for different plaque types with different mechanisms predominant for each classification.

The diameter of the samples used for mechanical testing was of a similar order of magnitude to the inhomogeneity observed in the tissue using both duplex ultrasound imaging and macroscopic visual observation. However, due to the resolution of the imaging used it is possible that smaller inhomogeneities such as micro-calcifications were not identified. Therefore, the test data provides global tissue mechanical properties

specific to the local clinical classifications that can be made using duplex ultrasound.

There are a number of limitations to the testing protocol adopted in this study. The mechanical testing was performed at room temperature rather than a more biologically appropriate 37 °C. The data-fitting procedure assumes that homogeneous deformation occurs when the tissue is loaded uniaxially. Given that atherosclerotic plaque has been seen to exhibit anisotropic behavior[18] it is likely that the deformation would be inhomogeneous when loaded. Limitations of tissue availability and local variations in the mechanical properties of atherosclerotic plaques[28] prevented the use of the larger sample sizes needed for uniaxial or biaxial tensile testing, and as a result unconfined uniaxial compressive testing was performed on plaque samples. As the major loading during the course of balloon angioplasty is circumferential tensile, this represents a notable limitation to the present study if using the data for modeling such clinical procedures. Understanding the relative contributions of radial and circumferential stresses in determining permanent deformation and stress softening during angioplasty is complicated by the fact that the plaque tissue itself is inhomogeneous, typically consisting of islands of stiffer tissue surrounded by more compliant tissue. This results in a differing multi-axial stress state locally in regions near the interface between the tissue components particularly where there are large differences in the stiffness of the components, potentially increasing the importance of radial stresses locally in the tissue. The overall importance of this effect on the radial compressive stresses within the tissue will most likely increase with increasing plaque inhomogeneity. Regardless evaluating the radial compressive behavior alone is not sufficient to develop a complete constitutive model for predicting lumen gain during angioplasty, although it could be argued that a constitutive model of inelasticity based on such data is an improvement on the use of purely elastic FE models which currently dominate the stent–artery interaction literature.[5,9,10,21,30,37,50] This argument is partially motivated by the observation in our previous study[28] that human plaque tissue does not display dramatic tension–compression nonlinearity. Therefore, a constitutive model developed with this data would be capable of describing the initial loading behavior of plaque with comparable accuracy to current isotropic hyperelastic models, and provides an initial, albeit limited, estimate of stress softening and permanent deformation on unloading. If future testing reveals significant tension–compression nonlinearity in the levels of stress softening and permanent deformation then clearly this data, by itself, will not be suitable for use in modeling clinical procedures such angioplasty and stenting. Further studies are required to determine the inelastic properties of plaque following uniaxial and biaxial tensile testing. Coupling such data with FE modeling that considers the inhomogeneous nature of plaque tissue will allow the tissue to be more completely characterized.

It is possible that the compressive testing is capturing poro- or visco-elastic effects rather than a permanent inelastic strain effect. A preliminary study performed on porcine arterial tissue revealed little tissue recovery following dwell periods of up to 2 h. As the tissue was hydrated throughout the course of the test some recovery in mechanical properties would be expected if the reported "permanent" deformation was due in a large part to visco- or poro-elasticity of the material. Another challenge with testing biological tissue is ensuring uniform contact with the sample prior to the application of loading. Typically samples had a slightly uneven surface following removal. The magnitude of the preload in this study was chosen to ensure reasonably uniform contact with the specimen while minimizing the strain applied to the tissue.

There is currently little data available in the literature relating to the precise mechanisms of damage within atherosclerotic plaque on unloading. Mechanisms of lumen gain during angioplasty described clinically include plaque compression, fracture, and dissection among others.[19,46] Plaque composition varies between the different classifications, so it is possible that dissimilar mechanisms are at work in each plaque type. Due to the likelihood of differing mechanisms of damage at work in each classification, and without sufficient evidence for the mechanisms involved, a more general phenomenological model was presented to describe the inelastic phenomena observed due to compressive loading in all plaque classifications as an initial step toward the characterization of the tissue inelasticity. This model is a simple method of representing the test data, and the strain energy constants provided by the model facilitate dissemination of the experimental findings.

The constitutive model proposed in this study results in a consistent quality fit, see Fig. 4 and Table 2. The load envelope was assumed to be equivalent to the uniaxial loading behavior of the plaque. Ideally, the initial loading behavior of the plaque should be determined from a separate uniaxial compression test. However, due to high inter-sample variations in plaque mechanical properties observed in a given classification, it was not possible to combine the results of separate tests for loading and unloading. High variability in the standard deviations in the constants a and b result from the highly variable stiffness of the loading response. As the levels of permanent deformation are similar in plaques of varying

stiffness it is necessary that there is high variability in the variable c^*. It should be noted that despite C^* only being updated on unloading inelastic effects develop in tissue during the loading phase. In this model, the effects of damage during the initial loading is incorporated into the constants of the load envelope a and b, while the inelastic constants c^*, ζ_∞, and i represent the differences between the loading and unloading–reloading behavior of the tissue that occurs as a result of the inelasticity. The inelastic constants, ζ_∞ and i, were fit to the stress–strain response in the second loading cycle of each strain level. This decision was motivated by an interest in investigating repeated loading events of the lesion such as pre-stenting expansion by a balloon, stenting followed by post-stenting balloon expansion; as well as the effects of physiological loading of the lesion post-stenting due to movement.[38,45] The stress–strain response on unloading could have been used for the fit of ζ_∞ and i instead which would be of greater benefit to FE models in which only one loading–unloading cycle was present. Regardless the proposed model is more appropriate than the assumption of elasticity in determining the unloading behavior of the plaque, particularly as stress softening phenomena observed during the first unloading cycle were more significant than hysteresis effects in subsequent loading and unloading cycles.

There are a number of limitations associated with the proposed constitutive model of plaque inelasticity. The main limitation of the model is the assumption of isotropy. The damage is isotropic and uses the maximum value of the strain energy W_{IL} in its criteria for damage evolution. Therefore, only one type of loading regime can be adequately accounted for. If, for example, the tissue is loaded in compression in a given loading cycle and in tension in a subsequent loading cycle, damage will not progress unless the strain energy W_{IL} reaches a greater value in tension than it obtained in the compression, which is not necessarily the case in reality. In the case of stenting procedures where pre- or post-expansion is used the loading mechanism on the tissue will be similar in each loading phase allowing models of inelasticity similar to that proposed here to be used. For models that include different loading regimes such as bending or torsion that occur in peripheral arteries[45] an anisotropic inelastic model would need to be implemented.[13] The loading behavior defined by Eq. (3) is also isotropic. Further potential limitations include the fact that residual stresses and strains were not considered as part of the constitutive formulation. This is in line with the observation of approximately zero opening angles for atherosclerotic plaques cut longitudinally.[1] A rate-independent approach to plasticity and damage has also been assumed, however, rate dependency cannot be ruled out without further testing.

In conclusion, this study investigated aspects of the inelastic response of carotid atherosclerotic plaques to radial compression in order to obtain a better understanding of plaque response to loading. This study also aimed to relate the inelastic mechanical properties to plaque classification, finding no significant difference between the magnitudes of residual strains between each classification. Further testing is still required in order to adequately describe atherosclerotic plaque response to other modes of loading that plaque will experience during angioplasty. Due to the limitations discussed earlier caution should be used when implementing the model, which is based solely on compressive testing data alone, to make predictions of lumen gain during clinical procedures. However, the data presented here can be combined with tensile data from future studies to more fully describe the tissue response. As such this study can be viewed as an initial step toward the complete characterization of the inelastic response of atherosclerotic plaque to mechanical loading.

ACKNOWLEDGMENTS

This material is based on works supported by the Science Foundation Ireland under Grant No. 07/RFP/ENMF660.

REFERENCES

[1]Auer, M., R. Stollberger, P. Regitnig, F. Ebner, and G. A. Holzapfel. In vitro angioplasty of atherosclerotic human femoral arteries: analysis of the geometrical changes in the individual tissues using MRI and image processing. *Ann. Biomed. Eng*. 38:1276–1287, 2010.

[2]Balzani, D., J. Schroder, and D. Gross. Simulation of discontinuous damage incorporating residual stresses in circumferentially overstretched atherosclerotic arteries. *Acta Biomater*. 2:609–618, 2006.

[3]Barrett, S. R., M. P. Sutcliffe, S. Howarth, Z. Y. Li, and J. H. Gillard. Experimental measurement of the mechanical properties of carotid atherothrombotic plaque fibrous cap. *J. Biomech*. 41(9):1995–2002, 2009.

[4]Calvo, B., E. Pena, M. A. Martinez, and M. Doblare. An uncoupled directional damage model for fibred biological soft tissues. Formulation and computational aspects. *Int. J. Numer. Methods Eng*. 69:2037–2057, 2007.

[5]Chua, S. N. D., B. J. MacDonald, and M. S. J. Hashmi. Finite element simulation of slotted tube (stent) with the presence of plaque and artery by balloon expansion. *J. Mater. Process. Technol*. 155–156:1772–1779, 2004.

[6]Delfino, A., N. Stergiopulos, J. E. Moore, Jr., and J. J. Meister. Residual strain effects on the stress field in a thick

wall finite element model of the human carotid bifurcation. *J. Biomech.* 30:777–786, 1997.
[7]Diani, J., M. Brieu, and J. M. Vacherand. A damage directional constitutive model for Mullins effect with permanent set and induced anisotropy. *Eur. J. Mech. A Solids* 25:483–496, 2006.
[8]Dorfmann, A., and R. W. Ogden. A constitutive model for the Mullins effect with permanent set in particle-reinforced rubber. *Int. J. Solids Struct.* 41:1855–1878, 2004.
[9]Early, M., and D. J. Kelly. The role of vessel geometry and material properties on the mechanics of stenting in the coronary and peripheral arteries. *Proc. Inst. Mech. Eng. H* 224:465–476, 2010.
[10]Early, M., C. Lally, P. J. Prendergast, and D. J. Kelly. Stresses in peripheral arteries following stent placement: a finite element analysis. *Comput. Methods Biomech. Biomed. Eng.* 12:25–33, 2009.
[11]Ebenstein, D. M., D. Coughlin, J. Chapman, C. Li, and L. A. Pruitt. Nanomechanical properties of calcification, fibrous tissue, and hematoma from atherosclerotic plaques. *J. Biomed. Mater. Res. A* 91:1028–1037, 2009.
[12]Emery, J. L., J. H. Omens, and A. D. McCulloch. Strain softening in rat left ventricular myocardium. *J. Biomech. Eng.* 119:6–12, 1997.
[13]Gasser, T. C., and G. A. Holzapfel. A rate-independent elastoplastic model for biological fiber-reinforced composites at finite strains: continuum basis, algorithmic formulation and finite element implementation. *Comput. Mech.* 29:340–360, 2002.
[14]Gasser, T. C., and G. A. Holzapfel. Finite element modeling of balloon angioplasty by considering overstretch of remnant non-diseased tissues in lesions. *Comput. Mech.* 40:47–60, 2007.
[15]Gil, R., C. Di Mario, F. Prati, C. von Birgelen, P. Ruygrok, J. R. Roelandt, and P. W. Serruys. Influence of plaque composition on mechanisms of percutaneous transluminal coronary balloon angioplasty assessed by ultrasound imaging. *Am. Heart J.* 131:591–597, 1996.
[16]Hokanson, J., and S. Yazdani. A constitutive model of the artery with damage. *Mech. Res. Commun.* 24:151–159, 1997.
[17]Holzapfel, G. A. Nonlinear Solid Mechanics. New York: John Wiley & Sons, 2000.
[18]Holzapfel, G. A., G. Sommer, and P. Regitnig. Anisotropic mechanical properties of tissue components in human atherosclerotic plaques. *J. Biomech. Eng.* 126:657–665, 2004.
[19]Honye, J., D. J. Mahon, A. Jain, C. J. White, S. R. Ramee, J. B. Wallis, A. al-Zarka, and J. M. Tobis. Morphological effects of coronary balloon angioplasty in vivo assessed by intravascular ultrasound imaging. *Circulation* 85:1012–1025, 1992.
[20]Kiousis, D. E., T. C. Gasser, and G. A. Holzapfel. A numerical model to study the interaction of vascular stents with human atherosclerotic lesions. *Ann. Biomed. Eng.* 35:1857–1869, 2007.
[21]Lally, C., F. Dolan, and P. J. Prendergast. Cardiovascular stent design and vessel stresses: a finite element analysis. *J. Biomech.* 38:1574–1581, 2005.
[22]Lee, R. T., A. J. Grodinsky, and E. H. Frank. Structure-dependent dynamic mechanical behavior of fibrous caps from human atherosclerotic plaques. *Circulation* 83:1764–1770, 1991.
[23]Lee, R. T., S. G. Richardson, H. M. Loree, A. J. Grodinsky, S. A. Gharib, F. J. Schoen, and N. Pandian. Prediction of mechanical properties of human atherosclerotic tissue by high-frequency intravascular ultrasound imaging. An in vitro study. *Arterioscl. Thromb. Vasc. Biol.* 12:1–5, 1992.
[24]Li, J., D. Mayau, and V. Lagarrigue. A constitutive model dealing with damage due to cavity growth and the Mullins effect in rubber-like materials under triaxial loading. *J. Mech. Phys. Solids* 56:933–973, 2008.
[25]Li, D., and A. M. Robertson. A structural multi-mechanism damage model for cerebral arterial tissue. *J. Biomech. Eng.* 131:101013, 2009.
[26]Liang, D. K., D. Z. Yang, M. Qi, and W. Q. Wang. Finite element analysis of the implantation of a balloon-expandable stent in a stenosed artery. *Int. J. Cardiol.* 104:314–318, 2005.
[27]Loree, H. M., A. J. Grodinsky, S. Y. Park, L. J. Gibson, and R. T. Lee. Static circumferential tangential modulus of human atherosclerotic tissue. *J. Biomech.* 27:195–204, 1994.
[28]Maher, E., A. Creane, S. Sultan, N. Hynes, C. Lally, and D. J. Kelly. Tensile and compressive properties of fresh human carotid atherosclerotic plaques. *J. Biomech.* 42:2760–2767, 2009.
[29]Miehe, C. Discontinuous and continuous damage evolution in Ogden-type large-strain elastic materials. *Eur. J. Mech. A Solids* 14:697–720, 1995.
[30]Migliavacca, F., L. Petrini, P. Massarotti, S. Schievano, F. Auricchio, and G. Dubini. Stainless and shape memory alloy coronary stents: a computational study on the interaction with the vascular wall. *Biomech. Model. Mechanobiol.* 2:205–217, 2004.
[31]Mortier, P., G. A. Holzapfel, M. De Beule, D. Van Loo, Y. Taeymans, P. Segers, P. Verdonck, and B. Verhegghe. A novel simulation strategy for stent insertion and deployment in curved coronary bifurcations: comparison of three drug-eluting stents. *Ann. Biomed. Eng.* 38:88–99, 2010.
[32]Naghdi, P. M., and J. A. Tarpp. The significance of formulating plasticity theory with reference to loading surfaces in strain space. *Int. J. Eng. Sci.* 13:785–797, 1975.
[33]Nicolaides, A. N., S. K. Kakkos, M. Griffin, G. Geroulakos, and E. Bashardi. Ultrasound plaque characterisation, genetic markers and risks. *Pathophysiol. Haemost. Thromb.* 32:371–377, 2002.
[34]Ogden, R. W., and D. G. Roxburgh. A pseudo-elastic model for the Mullins effect in filled rubber. *Proc. R. Soc. Lond. A* 455:2861–2877, 1999.
[35]Pena, E., B. Calvo, M. A. Martinez, and M. Doblare. On finite-strain damage of viscoelastic-fibred materials. Applications to soft biological tissues. *Int. J. Numer. Methods Eng.* 74:1198–1218, 2008.
[36]Pena, E., and M. Doblare. An anisotropic pseudo-elastic approach for modelling Mullins effect in fibrous biological materials. *Mech. Res. Commun.* 36:784–790, 2009.
[37]Pericevic, I., C. Lally, D. Toner, and D. J. Kelly. The influence of plaque composition on underlying arterial wall stress during stent expansion: the case for lesion-specific stents. *Med. Eng. Phys.* 31:428–433, 2009.
[38]Robertson, S. W., C. P. Cheng, and M. K. Razavi. Biomechanical response of stented carotid arteries to swallowing and neck motion. *J. Endovasc. Ther.* 15:663–671, 2008.
[39]Simo, J. C., and J. W. Ju. Strain- and stress-based continuum damage models—II. Computational aspects. *Int. J. Solids Struct.* 7:841–869, 1987.

[40]Tanaka, E., and H. Yamada. Inelastic constitutive modeling for blood vessels based on viscoplasticity. *Front. Med. Biol. Eng.* 2:177–180, 1990.
[41]Tegos, T. J., K. J. Alomiris, M. M. Sabetai, E. Kalodiki, and A. N. Nicolaides. Significance of sonographic tissue and surface characteristics of carotid plaques. *Am. J. Neuroradiol.* 22:1605–1612, 2001.
[42]Topoleski, L. D., and N. V. Salunke. Mechanical behavior of calcified plaques: a summary of compression and stress-relaxation experiments. *Z. Kardiol.* 89(Suppl 2):85–91, 2000.
[43]Topoleski, L. D. T., N. V. Salunke, and W. J. Mergner. Composition- and history-dependent radial compressive behavior of human atherosclerotic plaque. *J. Biomed. Mater. Res.* 35:117–127, 1997.
[44]Volokh, K. Y., and D. A. Vorp. A model of growth and rupture of abdominal aortic aneurysm. *J. Biomech.* 41: 1015–1021, 2008.
[45]Vos, A. W., M. A. Linsen, J. T. Marcus, J. C. van den Berg, J. A. Vos, J. A. Rauwerda, and W. Wisselink. Carotid artery dynamics during head movements: a reason for concern with regard to carotid stenting? *J. Endovasc. Ther.* 10:862–869, 2003.
[46]Waller, B. F. The eccentric coronary atherosclerotic plaque: morphologic observations and clinical relevance. *Clin. Cardiol.* 12:14–20, 1989.
[47]Woo, C., W. Kinm, and J. Kwon. A study on the material properties and fatigue life prediction of natural rubber component. *Mater. Sci. Eng. A* 483–484:376–381, 2008.
[48]Wu, W., M. Qi, X. P. Liu, D. Z. Yang, and W. Q. Wang. Delivery and release of nitinol stent in carotid artery and their interactions: a finite element analysis. *J. Biomech.* 40:3034–3040, 2007.
[49]Wulandana, R., and A. M. Robertson. An inelastic multi-mechanism constitutive equation for cerebral arterial tissue. *Biomech. Model. Mechanobiol.* 4:235–248, 2005.
[50]Zahedmanesh, H., D. John Kelly, and C. Lally. Simulation of a balloon expandable stent in a realistic coronary artery—determination of the optimum modelling strategy. *J. Biomech.* 43:2126–2132, 2010.